学位論文

The acidic domain of Hmga2 and the domain's linker region are critical for driving self-renewal of hematopoietic stem cell

（Hmga2 の酸性ドメインとそのリンカー領域は造血幹細胞の自己複製を促進する）

孫　宇奇

Sun Yuqi

熊本大学大学院医学教育部博士課程医学専攻白血病転写制御学

指導教員

指田　吾郎　教授

熊本大学大学院医学教育部博士課程医学専攻白血病転写制御学

2022年3月

学　位　論　文

Title of Thesis : **The acidic domain of Hmga2 and the domain’s linker region are critical for driving self-renewal of hematopoietic stem cell**
（Hmga2 の酸性ドメインとそのリンカー領域は造血幹細胞の自己複製を促進する）

Name of Autho : Sun Yuqi

Name of supervisor : Professor Sashida goro
Department of Transcriptional Regulation in Leukemogenesis, Medical Sciences Major, Doctoral Course of the Graduate School of Medical Sciences

Name of examiner : Professor Matsui Hirotaka Department of Molecular Laboratory Medicine

Professor Takizawa Hitoshi Department of Stem Cell stress

Professor Miharada Kenichi Department of Proteostasis in Stem cell

Associate Professor Hino shinjiro Department of Medical Cell Biology

March 2022

The acidic domain of Hmga2 and the domain's linker region are critical for driving self-renewal of hematopoietic stem cell

Yuqi Sun[1], Sho Kubota[1], Mihoko Iimori[1], Ai Hamashima[1], Haruka Murakami[1], Jie Bai[1], Mariko Morii[1], Takako Yokomizo-Nakano[1], Motomi Osato[2], Kimi Araki[3,4], and Goro Sashida[1]

1 Laboratory of Transcriptional Regulation in Leukemogenesis, International Research Center for Medical Sciences (IRCMS), Kumamoto University, Kumamoto, Japan; 2 Cancer Science Institute of Singapore, National University of Singapore, Singapore; 3 Institute of Resource Development and Analysis, Kumamoto University, Kumamoto, Japan; 4 Center for Metabolic Regulation of Healthy Aging, Kumamoto University, Kumamoto, Japan.

Running title: Hmga2 C-terminus region regulates stem cell function.

Keywords: Hmga1, AT-hook, Igf2bp2, Rosa26, and Conditional knock-in

Disclosure: The authors declare no competing interests.

Manuscript type: Original article.

Corresponding Author:

Goro Sashida, MD, PhD

2-2-1 Honjo, Chuo-ku, Kumamoto 860-0811, Japan

Phone: +81-96-373-6827

Fax: +81-96-373-6869

E-mail: sashidag@kumamoto-u.ac.jp

Abstract

High mobility group AT-hook 2 (Hmga2) is a chromatin modifier protein that plays a critical role in fetal development and leukemia propagation by binding to chromatin and DNA via its AT-hook domains. However, the molecular mechanisms by which Hmga2 activates the expression of target genes to drive the self-renewal of hematopoietic stem cells (HSCs) remain unclear. We generated *Rosa26* locus *Hmga2* conditional knock-in mice and found that overexpression of Hmga2 promoted self-renewal of normal HSCs, but maintained their fitness in bone marrow, and consequently was not sufficient to initiate malignancy. This result is consistent with previous findings showing that Hmga2 is a proto-oncogene. We also assessed the cellular functions of Hmga2 mutants lacking functional domains and demonstrated that the C-terminus acidic domain of Hmga2 and the domain's linker region were critical for activating genes involved in stem cell signatures, such as the *Igf2bp2* gene, to drive proliferation of HSCs. In contrast, overexpression of Hmga1, a member of the Hmga family with a different linker region, did not drive proliferation of HSCs. Our results reveal a critical role for the acidic domain of Hmga2 and the domain's linker region in modulating the transcription and self-renewal functions of HSCs.

Introduction

High mobility group (HMG) proteins are non-histone chromosomal proteins that are classified into three subtypes: HMGA, HMGB, and HMGN. The HMGA (High mobility group AT-hook) family is composed of four proteins: HMGA1a, HMGA1b, HMGA1c, and HMGA2, which bind to the minor groove of the AT-rich sequences of DNA through three AT-hook domains in the N-terminus and mediate various functions on DNA for transcription, replication, and repair (1,2). HMGA proteins contain the C-terminus acidic domain, which may modulate transcriptional properties via its structural flexibility based on previous findings on the acidic domains of HMGB proteins (3,4). HMGA proteins have also been shown to open compacted chromatin by competing with linker-histone H1 in order to activate the transcription of target genes. Hmga2 expression is robustly elevated by the Lin28b-Let-7 axis in fetal hematopoietic stem cells (HSCs), being higher than that in adult HSCs, but is suppressed during the differentiation by polycomb repressive complexes 2 (5). The ectopic expression of *Hmga2* by a retrovirus vector enhanced the self-renewal capacity of HSCs, but also promoted the production of megakaryocytes and erythroid cells in adult hematopoiesis (6,7). The constitutive activation of Hmga2 was consistently induced in a transgenic mouse model of *Hmga2* cDNA lacking the 3' untranslated region (UTR), which contained the Let-7 miRNA target sequences, and a mild myeloproliferative phenotype was observed (8). We recently demonstrated that the ectopic expression of *Hmga2* retrovirally in HSCs did not result in the development of malignancies in mice, whereas *Hmga2*-overexpressing *Tet2*-deficient mice showed the enhanced proliferation of hematopoietic stem and progenitor cells (HSPCs), which ultimately led to myeloid malignancies (9). The overexpression of Hmga2 increased the self-renewal capacity of both normal and malignant stem cells; however, the molecular mechanisms by which Hmga2 drives the self-renewal capacity of HSCs have not yet been elucidated.

To clarify the functions of Hmga2 in HSCs, we initially generated a new conditional knock-in (KI) of *Hmga2* cDNA that lacks its 3'UTR to the *Rosa* 26 locus in mice and then investigated the molecular mechanisms by which domains and regions in the Hmga2 protein contribute to the transcriptional activation of stem cell genes, such as *Igf2bp2*. We herein demonstrated that the overexpression of Hmga2 promoted the expansion of stem cells, but maintained their fitness in bone marrow; therefore, it was not sufficient for the development of malignant diseases in mice. Since three AT-hooks in Hmga proteins were required for the appropriate regulation of Hmga2 for its binding

to and the transcription of target genes (10,11), the deletion of the first AT-hook compromised the activation of the *Igf2bp2* gene. Notably, we also showed that the C-terminus acidic domain and its linker region, comprising eleven amino acids, in Hmga2 were required for the full activation of *Igf2bp2* expression in order to drive the proliferation of HSCs *in vitro*.

Methods

Mice

The Rosa26-flox-stop-flox-HA-Hmga2-eGFP conditional KI mouse line was generated using C57BL/6 ES cells at the Institute of Resource of Development and Analysis, Kumamoto University. HA-tagged *Hmga2* cDNA lacking the 3'UTR, which was generated by PCR using the mRNA of wild-type murine fetal blood cells, was inserted into the STOP-eGFP-ROSA26TV vector gifted from Dr. Klaus Rajewsky (Addgene plasmid # 1173). Hmga2-KI mice and Rosa26-flox-stop-flox-EYFP KI mice (12) were crossed with enhancer of *Runx1*-CreERT2 (*eR1-CreERT2*) transgenic mice provided by Dr. Motomi Osato (13) or Rosa26 Cre-ERT2 KI mice (Taconic). Two milligrams of tamoxifen (T5648, Sigma-Aldrich) was intraperitoneally injected on 5 consecutive days to delete the floxed stop element. C57BL/6 mice congenic for the Ly5 locus (CD45.1) were purchased from Sankyo-Lab Service. All mice were maintained on the C57BL/6 background. Age-matched female mice were used for donors and recipients in transplantation experiments. All experiments using these mice were performed in accordance with our institutional guidelines for the use of laboratory animals and approved by the Review Board for Animal Experiments of Kumamoto University (Kumamoto, Japan).

Quantitative RT-PCR, genomic PCR, immunofluorescence (IF), and Western blotting

Total RNA was extracted using ISOGEN (Nippon Gene), and cDNA was synthesized using the ProtoScript II First Strand cDNA Synthesis Kit (New England Biolabs) with an oligo-dT primer. Quantitative-RT-PCR was performed on LightCycler 480 (Roche) using Luna Universal qPCR Master Mix (New England Biolabs). Expression levels were normalized to those of ACTB/β-actin. Primers for RT-PCR and genomic PCR are listed in Supplementary Table 1. IF was performed using the BDCytofix/Cytoperm™ Fixation/Permeabilization Kit (BD). IF and Western blotting used the following antibodies: Hmga2 (CST, 5269S), FLAG (Sigma, M2), DYKDDDDK tag (Wako, 1E6), HA (Santa Cruz, 12CA5), Histone H3 (Abcam, ab1791), and actin (Santa Cruz, C4).

Cells

293T and Jurkat cell lines were cultured in DMEM or RPMI1640 containing 10% fetal bovine serum (FBS), respectively, in a humidified incubator. The 293GPG cell line was kindly provided by Dr. Mulligan (14).

Retrovirus vectors and transduction

FLAG-tagged Hmga2 and Hmga1 cDNAs were inserted into the pGCDN-sam-IRES-NGFR retrovirus vector. Deletion mutants of Hmga2 were subcloned from the Hmga2 virus vector. Virus supernatant (VSV-G pseudotyped retroviral supernatant) was prepared by transfecting 293GPG cells with an empty control or the Hmga2 retrovirus vector plasmid using the calcium phosphate transfection method. Virus vector transduction was performed as previously described (15). Briefly, virus supernatant was concentrated by centrifugation and the titers of retroviral supernatants were assessed by utilizing the Jurkat cells. Hematopoietic cells isolated from male mice were infected with the virus supernatant in 10 μg/mL protamine sulfate and 10 ng/mL RetroNectin (Takara), and were further cultured in SF-03 medium (Iwai North America) supplemented with 1% FBS, 100 ng/mL mouse stem cell factor (SCF; PeproTech), and 100 ng/mL human thrombopoietin (TPO; PeproTech) (15).

Flow cytometry and antibodies

Flow cytometry and cell sorting were performed using the following antibodies (clone and catalogue numbers): CD45.2 (104, 109820), CD45.1 (A20, 110730), Gr1 (RB6-8C5, 108404), CD11b/Mac1 (M1/70, 101208), Ter119 (116204), CD127/IL-7Rα (A7R34, 121104), B220 (RA3-6B2, 103212), CD4 (L3T4, 100526), CD8α (53-6.7, 100714), CD117/c-Kit (2B8, 105812), Sca-1 (D7, 108114), CD34 (MEC14.7, 11-0341-85), CD150 (TC15-12F12.2, 115924), CD135 (A2F10, 135306), CD48 (HM48-1, 103433), CD41(MWReg30, 133915), FcγRII-III (93, 101308), and NGFR (ME20.4, 345110). These antibodies were purchased from BioLegend or eBioscience. The lineage mixture solution contained biotin-conjugated anti-Gr1, B220, CD4, CD8α, Ter119, and IL-7Rα antibodies. All flow cytometric analyses and cell sorting were performed on FACSAriaII or FACSCantoII (BD).

RNA sequencing

RNA isolation, cDNA library preparation and sequencing were performed as previously described (15). Kallisto (version 0.43.1) was used for read counts and the calculation of transcripts per million. RNA sequencing data have been deposited in the DDBJ under the accession number: DRA013143 (Supplementary Dataset 1).

Results

Hmga2 conditional KI mice showed the enhanced expression of Hmga2 in adult HSCs

To assess the cellular function of the overexpression of Hmga2 in adult HSCs, we selected the *Rosa26* locus to generate a new conditional KI mouse line carrying a heterozygous allele of *Rosa26-loxP-STOP-loxP-HA-tag-Hmga2-IRES-EGFP* (Figure 1A, 1B), the *Hmga2* cDNA sequence of which did not contain 3' UTR of the *Hmga2* gene harboring the Let7 miRNA target sequences. The established *Hmga2* KI mouse lines were crossed with *eR1-CreERT2* transgenic mice, which dominantly induced Cre recombinase expression in HSPCs upon the intraperitoneal administration of tamoxifen to mice (13). We confirmed the up-regulated expression of the Hmga2 protein in lineage$^-$c-Kit$^+$ bone marrow cells isolated from two *Hmga2* KI; *eR1-CreERT2* mouse lines (clone #30 and #33) one month after the treatment with tamoxifen, but negligible levels in wild-type counterpart cells using a Western blot analysis with the anti-HA or anti-Hmga2 antibody (Figure 1C). We subsequently examined clone #30. Quantitative-RT-PCR (Q-PCR) revealed that *Hmga2* KI HSCs had significantly increased expression of *Hmga2*, which was higher than that in wild-type fetal HSCs, while control HSCs showed a lower expression of *Hmga2* (Figure 1D). Therefore, we successfully generated *Hmga2* KI; *eR1-CreERT2* mice overexpressing Hmga2 at both the mRNA and protein levels in immature blood cells, including HSCs.

Hmga2 overexpression enhanced the hematopoiesis but maintained the fitness in bone marrow

To assess the blood cell-specific effects of the overexpression of Hmga2 in mice, we transplanted bone marrow cells isolated from *Hmga2* KI; *eR1-CreERT2* mice and *Rosa26-loxP-STOP-loxP-EYFP*; *eR1-CreERT2* mice, referred to as *YFP* KI mice, into lethally-irradiated congenic Ly5.1+ wild-type recipient mice. One month after transplantation, tamoxifen was intraperitoneally administered to mice for five days in order to induce the expression of Cre recombinase in blood cells (Figure 2A).

The induction efficacies of Hmga2-IRES-EGFP or EYFP in HSPCs in bone marrow 48 hours after a single injection of tamoxifen were examined using flow cytometry. Hmga2 KI cells showed similar induction efficacies in HSCs and multipotent progenitor (MPP1-4) cells (16) to those in YFP KI cells (Figure 2B). Ten months after transplantation, Hmga2 KI mice showed similar complete blood cell counts and proportions of myeloid and B- and T-lymphoid cells in peripheral blood (PB) to those in YFP KI mice (Figure 2C, 2D). Total BM cell numbers (Figure 2E) and HSCs and MPPs (MPP1-4) in BM were similar between Hmga2 KI mice and control YFP KI mice (Figure 2F); however, Hmga2 KI mice showed significantly higher frequencies of GFP-positive cells within HSCs, MPP1-4 and myeloid progenitor cells (17) than YFP-positive cells in control mice one year after transplantation (Figure 2G, 2H). Hmga2 KI mice consistently showed gradual and significant increases in GFP-positive cell proportions in myeloid cells, B cells, and platelets (Supplementary Figure 1), while control YFP KI mice sustained the YFP proportion in mature cells in PB and in HSCs in BM at similar levels to those observed in the initial induction period at 48 hours (Supplementary Figure 2). Based on extramedullary hematopoiesis in a Hmga2 transgenic mouse as previously reported (8), we performed phenotypic analyses on the spleen and liver in Hmga2 KI mice. Hmga2 KI mice showed similar weight of the spleen and liver to those in YFP KI mice (Figure 2I, 2J). Histological analyses revealed a very mild increase in the area of red pulp in the spleen of Hmga2 KI mice without the development of evident hematological malignancies (Figure 2K), thereby, we observed both genotype mice showed similar survival outcomes (Supplementary Figure 3). Therefore, the overexpression of Hmga2 promoted the hematopoiesis, but maintained the fitness in PB and BM in mice.

Hmga2 overexpression increased expression of Igf2bp2 target genes and enhanced the self-renewal capacity of stem cells

To assess the self-renewal capacity of Hmga2-over-expressing HSC, we performed serial transplantation using 1000 Lineage$^-$Sca-1$^+$c-Kit$^+$ (LSK) cells isolated from primary transplanted mice and freshly isolated 2x10^5 Ly5.1+ wild-type BM cells, and found that *Hmga2* KI; *Cre-ERT2* cells significantly increased the competitive repopulating capacities of HSPCs and myeloid progenitor cells over those of control *Cre-ERT2* cells (Figure 3A and Supplementary Figure 4). Thus, the overexpression of Hmga2 enhanced the self-renewal capacity of stem cells in an *in vivo* condition.

To elucidate the mechanisms underlying the enhanced self-renewal capacity of Hmga2-over-

expressing stem cells, we performed RNA sequencing analyses of $CD150^{+}CD48^{-}CD34^{-}CD135^{-}LSK$ HSCs isolated from *Hmga2* KI; *Cre-ERT2* mice and control *Cre-ERT2* mice 2 months after transplantation. We observed 326 up-regulated genes and 339 down-regulated genes by more than 2-fold change in Hmga2 KI HSCs from those in control HSCs (Supplementary Dataset 2). Among those up-regulated genes, since Hmga2 bound to a proximal region of *Igf2bp2* in HSPCs (9), we found that the expression levels of *Igf2bp2* mRNA in HSCs were significantly higher in Hmga2 KI mice than in control mice. Q-PCR confirmed the increased expression of *Igf2bp2* in Hmga2 KI HSCs, compared to control HSCs (Figure 3B). A gene set enrichment analysis (GSEA) consistently showed that in comparison with control HSCs, Hmga2 KI HSCs had significantly positive enrichments in Igf2bp2 target genes (Figure 3C), which were defined in K562 leukemic cells and 293T cancer cells (18)(19). IGF2BP2 has been shown to stabilize *MYC* mRNA and activate expression of MYC-target genes in epithelial cancer cells (19); however, Q-PCR revealed that Hmga2 KI HSCs showed similar expression of *Myc* mRNA to that in control HSCs (Figure 3D). By performing GSEA, we also found that in comparison with control HSCs, Hmga2 KI HSCs did not have significant changes in MYC hallmark target genes (Figure 3E), indicating that the activation of *Myc* and its target genes did not appear to contribute to the enhanced self-renewal of Hmga2 KI HSCs. Nonetheless, the over-expression of Hmga2 enhanced the self-renewal capacity of stem cells accompanied with enhanced expression of Igf2bp2 target genes.

Hmga2 mutants lacking N- and C-terminus domains were expressed in the nucleus

Hmga proteins harbor three AT-hook domains to bind to DNA and modulate the transcription of target genes, but differ in their linker regions (Figure 4A). To identify which domains of the Hmga2 protein are contributing to the competitive repopulation of HSCs, we generated truncated mutants of the Hmga2 protein by deleting either its N- or C-terminus, which were tagged by the FLAG sequence (Figure 4B). Hmga1, a member of the Hmga family, is expressed in adult HSCs (16). We also generated an expression vector of full-length Hmga1a cDNA harboring distinct sequences at linker regions between AT-hooks and the acidic domain (Figure 4A, 4B). The transfection of these mutants into 293T human kidney cells confirmed the clear induction of these Hmga2 mutants expressing the expected sizes of their proteins in transfected cells (Figure 4C). To assess the distribution of Hmga2-mutant proteins in cells, we performed IF assays using Hmga2 mutant-transduced Jurkat human

leukemia cells (Figure 4D). The IF assay revealed that all mutants of and wild-type Hmga2 and Hmga1 were dominantly expressed in the nucleus, whereas the Hmga2-Δ1-45 mutant lacking the first AT-hook showed markedly lower expression in cells, presumably due to its impaired affinity to chromatin and DNA.

Hmga2 overexpression required its N- and C-terminus domains to activate Igf2bp2

We then examined the cellular function of Hmga2 mutant-transduced HSCs under *in vitro* conditions supplemented with SCF and TPO to maintain the immature phenotype of hematopoietic cells. Consistent with previous findings showing the enhanced self-renewal property of Hmga2 in stem cells (20), the transduction of wild-type Hmga2 markedly increased the size of colonies and cell numbers, while that of Hmga1 did not increase cell numbers in a six-day culture, similar to cells transduced with the control empty vector (Figure 5A, 5B). We found that Hmga2-Δ1-45 lacking the first AT-hook and Hmga2-Δ83-108 lacking the C-terminus region did not expand cell numbers, while the Hmga2-Δ1-25 mutant and Hmga2-Δ94-108 lacking only the acidic domain induced the mild expansion of transduced HSCs (Figure 5A). These results indicated that the first AT-hook and the linker region (83-93aa) together with the acidic domain are required for the enhanced self-renewal property of Hmga2 in stem cells. The acidic domain promotes the expansion of HSCs and requires the linker regions for the further expansion of stem cells, at least under *in vitro* conditions.

In *in vitro* experiments using Hmga2 mutants, we observed similar *Hmga2* mRNA expression levels in all mutant-transduced blood cells (Figure 5C), which was consistent with the similar expression levels of Hmga2 mutant proteins transfected in 293T cells (Figure 4C). Consistent with the increased expression of *Igf2bp2* in Hmga2 KI HSCs (Figure 3B), we also showed that *Igf2bp2* expression levels were significantly higher in full-length Hmga2, Hmga2-Δ1-25, and Hmga2-Δ94-108 than in control cells; however, the increased expression of the *Igf2bp2* gene was abrogated in the Hmga2-Δ1-45 and Hmga2-Δ83-108 mutants (Figure 5D), leading to impairments in the expansion of stem cells transduced by these Hmga2 mutants lacking the N- or C-terminus (Figure 5A). AT-hook domains were highly conserved in the Hmga1 and Hmga2 proteins, whereas their linker regions differed (Figure 4A). The overexpression of Hmga1 did not up-regulate the expression of *Igf2bp2* in blood cells (Figure 5D), which supports the linker region at 83-93aa in the Hmga2 protein, which is not shared by the Hmga1 protein, being critical for the transcriptional activator property of Hgma2.

Therefore, the overexpression of Hmga2 required its three AT-hooks and the C-terminus linker region to activate the transcription of *Igf2bp2* and promote the self-renewal function of HSCs.

Discussion

In the present study, we successfully generated a new *Hmga2* conditional KI mouse with the up-regulated expression of the *Igf2bp2* gene, which is known to be highly expressed in fetal HSCs. IGF2BP2 recognizes m6A-modified RNAs to promote the stability and translation of target mRNAs and protect mRNAs from Let-7 miRNA-mediated degradation (21). In human cancer cells, HMGA2 has been shown to activate the transcription of *IGF2BP2/IMP2* (22), which functions as an oncogene to bind to and stabilize *MYC* mRNA and promote proliferation (19). We consistently demonstrated that Hmga2 bound to a proximal region of the *Igf2bp2* gene and activated the transcription of *Igf2bp2* in both normal and *Tet2*-null HSCs, thereby driving proliferation under *in vivo* and *in vitro* conditions (9). In this study, we demonstrated that the over-expression of Hmga2 did not activate expression of Myc target genes in wild-type HSCs. The enhanced expression of Myc protein is deleterious to normal HSCs (23,24), while the blood cell-specific deletion of *Myc* results in the expansion of HSCs in part due to blocking the differentiation (25). These findings highlight a context-dependent function of the Hmga2-Igf2bp2 axis for enhancing the self-renewal of normal and malignant stem cells. Further studies are needed to elucidate the mechanisms by which the Hmga2-Igf2bp2 axis regulates target genes and enhances the self-renewal capacity of normal HSCs in a Myc-independent manner.

A transgenic mouse carrying *Hmga2* cDNA lacking the 3'UTR showed myeloproliferative features including extramedullary hematopoiesis in the spleen (8,26), while we demonstrated that our *Rosa26* locus *Hmga2* conditional KI mice, in which *Hmga2* cDNA lacked the 3'UTR, showed a mild expansion of red pulp in the spleen without expansion of mature blood cells in the BM and in the PB, in comparison with the control mice. Those distinct phenotypes by the over-expression of *Hmga2* in two models would be caused by differences in a given time point (inducible versus constitutive) and in a tissue specificity (blood-specific versus whole body).

We demonstrated that the first AT-hook, the acidic domain, and its linker region at 83-93aa in Hmga2 were critical for activating the expression of *Igf2bp2* and enhancing the proliferation of HSCs. AT-hooks were previously shown to be important for the transcriptional activating property of Hmga2 (1,2), while the transcriptional activity of the linker region of Hmga2 remained largely unknown. In

contrast, the Hmga1 protein lacks the linker region including lysine residues, which may account for the distinct transcriptional activation of stem cell genes in a manner that is dependent on their conformational structures for binding to chromatin. Acidic domains were phosphorylated by casein kinase II in the Hmga2 protein, in which sites were shared in the Hmga1 protein showing different forms, which modulated DNA-binding capacity *in vitro* (27). This finding suggests a critical role for the linker region and the acidic domain in Hmga2 in modulating the transcription of target genes, presumably due to post-translational modifications in these regions and/or protein-protein interactions to form protein complexes in HSC in a context-dependent manner. The molecular mechanisms by which the acidic domain and linker region together modulate the DNA-binding property of the AT-hook domains of Hmga2, which activates the transcription of target genes in HSCs, will be examined in the future.

Acknowledgments

This work was supported in part by a grant from the Takeda Science Foundation (to G.S.), the Japanese Society of Hematology (to G.S.), Mochida Memorial Foundation for Medical and Pharmaceutical Research (to S.K.), Grants-in-Aid for Scientific Research (16KT0113, 18H02842, 19K08842, and 21H02952) from the Ministry of Education, Culture, Sports, Science and Technology (MEXT) of Japan, and Core-to-Core Program Advanced Research Networks "Integrative approach for normal and leukemic stem cells" from the Japan Society for the Promotion of Science (JSPS) of Japan. Yuqi Sun was supported by a scholarship from KOHNAN Asia Scholarship Foundation.

References

1. Fusco A, Fedele M. Roles of HMGA proteins in cancer. Nat Rev Cancer. 2007;7(12):899–910.
2. Cleynen I, Van de Ven WJM. The HMGA proteins: A myriad of functions. Int J Oncol. 2008;32(2):289–305.
3. Thomsen MS, Franssen L, Launholt D, Fojan P, Grasser KD. Interactions of the basic N-terminal and the acidic C-terminal domains of the maize chromosomal HMGB1 protein. Biochemistry. 2004;43(25):8029–37.
4. Malarkey CS, Churchill MEA. The high mobility group box: The ultimate utility player of a cell. Trends Biochem Sci. 2012;37(12):553–62.
5. Oshima M, Hasegawa N, Mochizuki-Kashio M, Muto T, Miyagi S, Koide S, et al. Ezh2 regulates the Lin28/let-7 pathway to restrict activation of fetal gene signature in adult hematopoietic stem cells. Exp Hematol. 2016;44(4):282-296.e3.
6. Rowe RG, Wang LD, Coma S, Han A, Mathieu R, Pearson DS, et al. Developmental regulation of myeloerythroid progenitor function by the Lin28b–let-7–Hmga2 axis. J Exp Med. 2016;213(8):1497–512.
7. Sashida G, Wang C, Tomioka T, Oshima M, Aoyama K, Kanai A, et al. The loss of Ezh2 drives the pathogenesis of myelofibrosis and sensitizes tumor-initiating cells to bromodomain inhibition. J Exp Med. 2016;213(8):1459–77.
8. Ikeda K, Mason PJ, Bessler M. 3'UTR-truncated Hmga2 cDNAcauses MPN-like hematopoiesis by conferring a clonal growth advantage at the level of HSC in mice. Blood. 2011;117(22):5860–9.
9. Bai J, Yokomizo-Nakano T, Kubota S, Sun Y, Kanai A, Iimori M, et al. Overexpression of Hmga2 activates Igf2bp2 and remodels transcriptional program of Tet2-deficient stem cells in myeloid transformation. Oncogene. 2021;40(8):1531–41.
10. Nagpal S, Ghosn C, DiSepio D, Molina Y, Sutter M, Klein ES, et al. Retinoid-dependent recruitment of a histone H1 displacement activity by retinoic acid receptor. J Biol Chem. 1999;274(32):22563–8.
11. Yie J, Liang S, Merika M, Thanos D. Intra- and intermolecular cooperative binding of high-mobility-group protein I(Y) to the beta-interferon promoter. Mol Cell Biol. 1997 Jul;17(7):3649–62.
12. Srinivas S, Watanabe T, Lin CS, William CM, Tanabe Y, Jessell TM, et al. Cre reporter strains produced by targeted insertion of EYFP and ECFP into the ROSA26 locus. BMC Dev Biol. 2001;1:4.
13. Abdallah MG, Niibori-Nambu A, Morii M, Yokomizo T, Yokomizo T, Ideue T, et al. RUNX1-ETO (RUNX1-RUNX1T1) induces myeloid leukemia in mice in an age-dependent manner. Leukemia. 2021 Jun;
14. Ory DS, Neugeboren BA, Mulligan RC. A stable human-derived packaging cell line for production of high titer retrovirus/vesicular stomatitis virus G pseudotypes. Proc Natl Acad Sci U S A. 1996;93(21):11400–6.
15. Yokomizo-Nakano T, Kubota S, Bai J, Hamashima A, Morii M, Sun Y, et al. Overexpression of RUNX3 represses RUNX1 to drive transformation of myelodysplastic syndrome. Cancer Res. 2020 Apr;80(12):2523–36.
16. Cabezas-Wallscheid N, Klimmeck D, Hansson J, Lipka DB, Reyes A, Wang Q, et al. Identification of regulatory networks in HSCs and their immediate progeny via integrated proteome, transcriptome, and DNA methylome analysis. Cell Stem Cell. 2014;15(4):507–22.
17. Pronk CJH, Rossi DJ, Månsson R, Attema JL, Norddahl GL, Chan CKF, et al. Elucidation of the Phenotypic, Functional, and Molecular Topography of a Myeloerythroid Progenitor Cell Hierarchy. Cell Stem Cell. 2007;1(4):428–42.
18. Dunham I, Kundaje A, Aldred SF, Collins PJ, Davis CA, Doyle F, et al. An integrated encyclopedia of DNA elements in the human genome. Nature. 2012;489(7414):57–74.
19. Huang H, Weng H, Sun W, Qin X, Shi H, Wu H, et al. Recognition of RNA N 6 -methyladenosine by IGF2BP proteins enhances mRNA stability and translation. Nat Cell Biol. 2018;20(3):285–95.
20. Copley MR, Babovic S, Benz C, Knapp DJHF, Beer PA, Kent DG, et al. The Lin28b-let-7-Hmga2 axis determines the higher self-renewal potential of fetal haematopoietic stem cells. Nat Cell Biol. 2013;15(8):916–25.
21. Degrauwe N, Schlumpf TB, Janiszewska M, Martin P, Cauderay A, Provero P, et al. The RNA Binding Protein IMP2 Preserves Glioblastoma Stem Cells by Preventing let-7 Target Gene Silencing. Cell Rep. 2016 May;15(8):1634–47.
22. Cleynen I, Brants JR, Peeters K, Deckers R, Debiec-Rychter M, Sciot R, et al. HMGA2 regulates

transcription of the Imp2 gene via an intronic regulatory element in cooperation with nuclear factor-κB. Mol Cancer Res. 2007;5(4):363–72.

23. Matsuoka S, Oike Y, Onoyama I, Iwama A, Arai F, Takubo K, et al. Fbxw7 acts as a critical fail-safe against premature loss of hematopoietic stem cells and development of T-ALL. Genes Dev. 2008;22(8):986–91.
24. Reavie L, Gatta G Della, Crusio K, Aranda-Orgilles B, Buckley SM, Thompson B, et al. Regulation of hematopoietic stem cell differentiation by a single ubiquitin ligase-substrate complex. Nat Immunol. 2010;11(3):207–15.
25. Laurenti E, Varnum-Finney B, Wilson A, Ferrero I, Blanco-Bose WE, Ehninger A, et al. Hematopoietic Stem Cell Function and Survival Depend on c-Myc and N-Myc Activity. Cell Stem Cell. 2008;3(6):611–24.
26. Ueda K, Ikeda K, Ikezoe T, Harada-Shirado K, Ogawa K, Hashimoto Y, et al. Hmga2 collaborates with JAK2V617F in the development of myeloproliferative neoplasms. Blood Adv. 2017;1(15):1001–15.
27. Sgarra R, Maurizio E, Zammitti S, Lo Sardo A, Giancotti V, Manfioletti G. Macroscopic differences in HMGA oncoproteins post-translational modifications: C-terminal phosphorylation of HMGA2 affects its DNA binding properties. J Proteome Res. 2009 Jun;8(6):2978–89.

Figure legends

Figure 1. Generation of conditional Hmga2 knock-in mice

A) Schematic illustration showing the Rosa26 loxP-Stop-loxP HA-tagged Hmga2 IRES-eGFP vector, wild-type allele, targeted allele, and Cre-excised allele. Arrows indicate primers (#1, #2, #3, and #4) for genomic PCR performed in panel B to detect the *Rosa26* locus knock-in of the vector.

B) Genomic PCR showing targeted alleles in the *Rosa26* locus together with the wild-type control. Arrow heads indicate expected PCR products (2167bp by #1 and #2, 6406bp by #3 and #4).

C) Expression levels of the Hmga2 protein in c-Kit+ bone marrow cells isolated from control eR1-CreERT2 mice and Hmga2 KI; eR1-CreERT2 mice (two clones: #30 and #33).

D) Expression levels of *Hmga2* mRNA in HSCs isolated from control eR1-CreERT2 mice and Hmga2 KI; eR1-CreERT2 mice and wild-type fetal liver HSCs (n=6-7) examined by quantitative-PCR. Bars show the mean ± SD, **p<0.01, and ***p<0.001. P-values were calculated by the Student's *t*-test.

Figure 2. Hmga2 knock-in mice enhanced the hematopoiesis, but did not develop malignancies

A) Transplantation assay using BM cells isolated from YFP KI mice and Hmga2 KI mice

B) Proportion of YFP+ or GFP+ cells in HSCs and MPP1-4 in BM (n=4) 48 hours after the administration of tamoxifen.

C) Complete blood cell counts (CBC) in the PB of YFP KI mice and Hmga2 KI mice (n=10) ten months after transplantation.

D) Proportions of Gr-1$^+$/CD11b$^+$ myeloid cells, B220$^+$ B cells, and CD4$^+$/CD8$^+$ T cells in white blood cells in the PB of YFP KI mice and Hmga2 KI mice (n=10) ten months after transplantation.

E) BM cell counts of YFP KI mice and Hmga2 KI mice (n=6-8) one year after transplantation.

F) Frequencies of HSC and MPP1-4 cells in BM (n=6-8) one year after transplantation.

G) Proportion of YFP+ or GFP+ cells in HSCs and MPP1-4 in the BM of YFP KI mice and Hmga2 KI mice (n=6-8) one year after transplantation.

H) Proportion of YFP+ or GFP+ cells in Pre GM, GMP, Pre MegE, Pre CFU-E, and MkP in the BM of YFP KI mice and Hmga2 KI mice (n=6-8) one year after transplantation.

I, J) Weight of liver and spleen in YFP KI mice and Hmga2 KI mice (n=6-8) one year after transplantation.

K) Histological analysis showing the spleen in YFP KI mice and Hmga2 KI mice observed by hematoxylin-eosin staining. Scale bars, 500μm.

B-J) Bars show the mean ± SD, *p<0.05 and ***p<0.001. P-values were calculated by the Student's *t*-test.

Figure 3. Hmga2 knock-in HSCs showed the enhanced expression of Igf2bp2 target genes

A) Proportion of control Cre-ERT2 or Hmga2 KI; Cre-ERT2 CD45.2$^+$ cells in HSCs and MPP1-4 cells in BM (n=4-5) four months after secondary transplantation.

B) Expression levels of *Igf2bp2* mRNA in HSCs in BM isolated from control mice and Hmga2 KI mice (n=4) and in wild-type fetal liver HSCs (n=3) examined by quantitative-PCR.

C) GSEA of IGF2BP2 target gene sets, which were defined by more than 3-fold down-regulated genes in knockdown of the *IGF2BP2* gene in K562 and 293T cell lines (linked in GSE80946, 80858 and 90686), in Hmga2 KI HSCs and control HSCs 2 months after transplantation.

D) Expression levels of *Myc* mRNA in HSCs in BM isolated from control Cre-ERT2 mice and Hmga2 KI; Cre-ERT2 mice (n=4) examined by quantitative-PCR.

E) GSEA of MYC hallmark target genes sets (V1 and V2) in Hmga2 KI HSCs and control HSCs 2 months after transplantation.

B, D) Bars show the mean ± SD, *p<0.05 and ***p<0.001. P-values were calculated by the Student's *t*-test.

Figure 4. Generation of Hmga2 mutants lacking the N- and C-terminus domains

A) Amino acid alignment of murine Hmga1a and Hmga2 proteins.

B) Illustration of Hmga1a, the wild type, and mutants of Hmga2 (i.e. Δ1-25, Δ1-45, Δ83-108, and Δ94-108) showing the levels of conservation in sequences by distinct colors.

C) Expression levels of the wild type or deletion mutants of Hmga2 and Hmga1a in 293T cells examined by Western blotting using anti-FLAG and anti-actin antibodies. Actin was used as a loading control.

D) IF showing the expression of the wild type or deletion mutants of Hmga2 and Hmga1a transduced in Jurkat leukemia cells examined using an anti-FLAG antibody. DNA was counterstained by DAPI.

Figure 5. N- and C-terminus domains of Hmga2 were both required to activate Igf2bp2 and promote the expansion of HSCs

A) Cell counts of wild-type and mutant Hmga2-transduced HSCs after six days in liquid culture.

B) Representative pictures of Hmga2- and empty vector-transduced cells. Scale bars, 1mm.

C, D) Expression levels of *Hmga2* and *Igf2bp2* in wild-type and mutant Hmga2-transduced HSCs after six days in liquid culture examined by quantitative-PCR.

A, C, D) Bars show the mean ± SD, *p<0.05, **p<0.01, and ***p<0.001. n.s. stands for not significant. P-values were calculated by the Student's *t*-test.

Supplementary information

Supplementary Table 1

Sequences of primes for q-RT-PCR and genomic PCR.

Supplementary Figure 1

Proportions of YFP+ or GFP+ cells in Gr-1$^+$/CD11b$^+$ myeloid cells, B220$^+$ B cells, CD4$^+$/CD8$^+$ T cells, and CD41$^+$ platelets in the PB of YFP KI mice and Hmga2 KI mice (n=3-5) 9 months after transplantation.

Supplementary Figure 2

Proportion of YFP+ or GFP+ cells in HSCs and MPP1-4 cells in the BM of YFP KI mice and Hmga2 KI mice (n=4-8) 48 hours (48H) and twelve months (12M) after the tamoxifen treatment.

Supplementary Figure 3

Similar median survivals of YFP KI mice and Hmga2 KI mice after transplantation.

Supplementary Figure 4

Proportion of control Cre-ERT2 or Hmga2 KI; Cre-ERT2 CD45.2$^+$ cells in Pre GM, GMP, Pre MegE, Pre CFU-E, and MkP, in BM (n=4) four months after secondary transplantation.

Supplementary Figure 5

Un-cropped images of PCR gel and Western blotting.

Supplementary Dataset 1

RNA sequencing data list liked in DRA013143.

Supplementary Dataset 2

Up- and down-regulated genes in Hmga2 KI; Cre-ERT2 HSCs from those in control Cre-ERT2 HSCs.

Figure 1

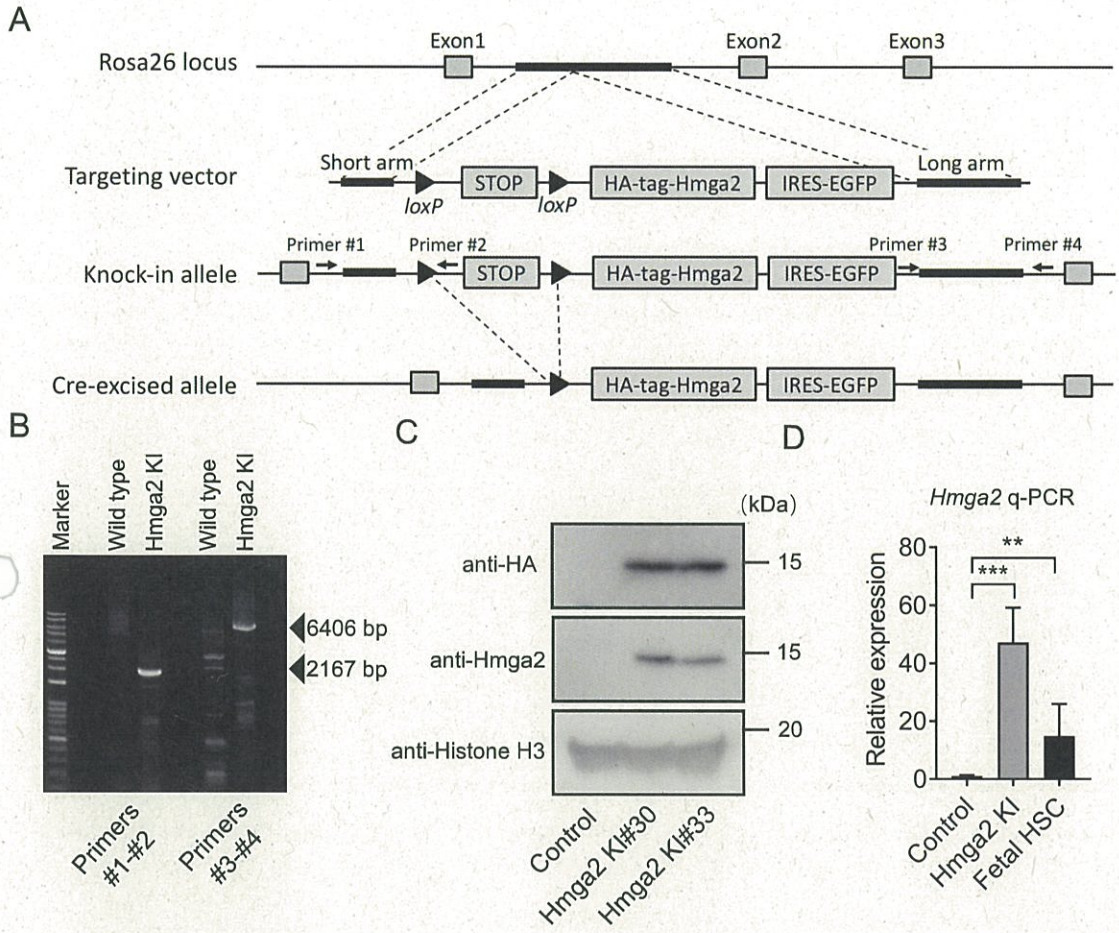
A
Rosa26 locus
Exon1
Exon2
Exon3
Targeting vector
Short arm
STOP
HA-tag-Hmga2
IRES-EGFP
Long arm
loxP
loxP
Primer #1
Primer #2
Primer #3
Primer #4
Knock-in allele
Cre-excised allele
B
Marker
Wild type
Hmga2 KI
Wild type
Hmga2 KI
6406 bp
2167 bp
Primers #1-#2
Primers #3-#4
C
(kDa)
anti-HA
anti-Hmga2
anti-Histone H3
15
15
20
Control
Hmga2 KI#30
Hmga2 KI#33
D
Hmga2 q-PCR
Relative expression
80
60
40
20
0
**
***
Control
Hmga2 KI
Fetal HSC

Figure 2

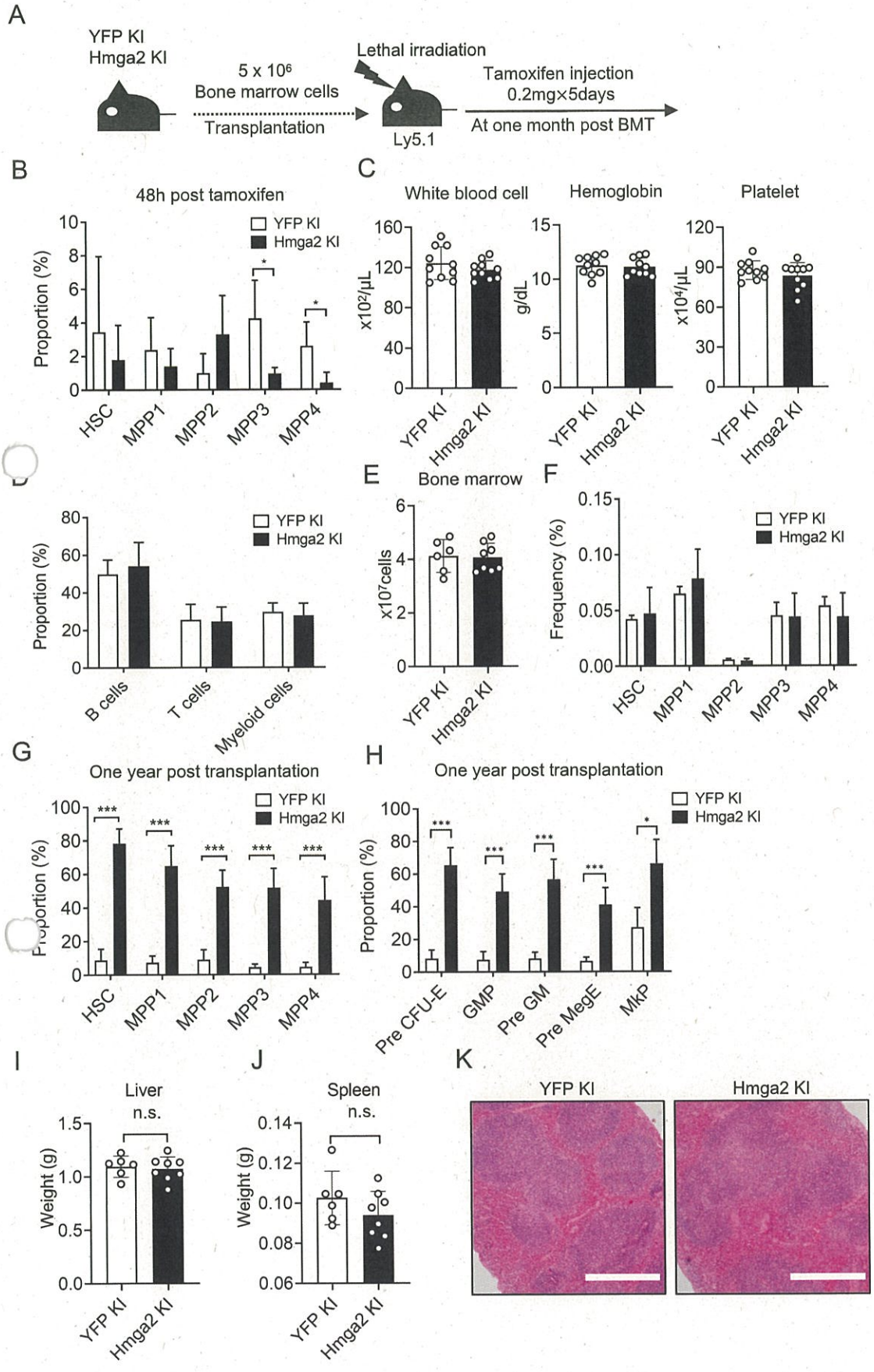
A
YFP KI
Hmga2 KI
5 x 10⁶
Bone marrow cells
Transplantation
Lethal irradiation
Ly5.1
Tamoxifen injection
0.2mg×5days
At one month post BMT
B
48h post tamoxifen
Proportion (%)
YFP KI
Hmga2 KI
HSC
MPP1
MPP2
MPP3
MPP4
C
White blood cell
Hemoglobin
Platelet
x10²/μL
g/dL
x10⁴/μL
D
Proportion (%)
B cells
T cells
Myeloid cells
E
Bone marrow
x10⁷cells
F
Frequency (%)
G
One year post transplantation
H
One year post transplantation
Pre CFU-E
GMP
Pre GM
Pre MegE
MkP
I
Liver
n.s.
Weight (g)
J
Spleen
n.s.
K

Figure 3

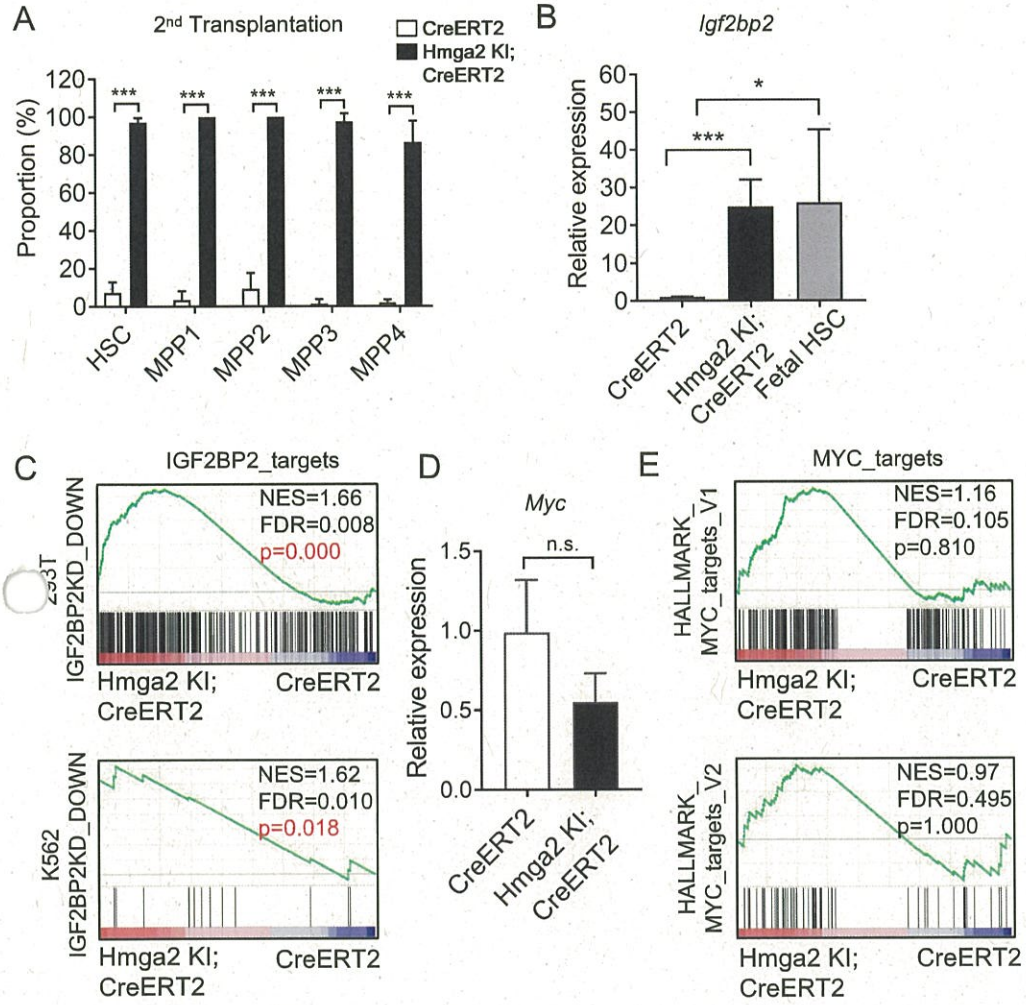
A
2nd Transplantation
CreERT2
Hmga2 KI; CreERT2
Proportion (%)
120
100
80
60
40
20
0
***
HSC
MPP1
MPP2
MPP3
MPP4
B
Igf2bp2
Relative expression
60
50
40
30
20
10
0
*
***
CreERT2
Hmga2 KI; CreERT2
Fetal HSC
C
IGF2BP2_targets
293T IGF2BP2KD_DOWN
NES=1.66
FDR=0.008
p=0.000
Hmga2 KI; CreERT2
CreERT2
K562 IGF2BP2KD_DOWN
NES=1.62
FDR=0.010
p=0.018
Hmga2 KI; CreERT2
CreERT2
D
Myc
Relative expression
1.5
1.0
0.5
0.0
n.s.
CreERT2
Hmga2 KI; CreERT2
E
MYC_targets
HALLMARK_ MYC_targets_V1
NES=1.16
FDR=0.105
p=0.810
Hmga2 KI; CreERT2
CreERT2
HALLMARK_ MYC_targets_V2
NES=0.97
FDR=0.495
p=1.000
Hmga2 KI; CreERT2
CreERT2

Figure 4

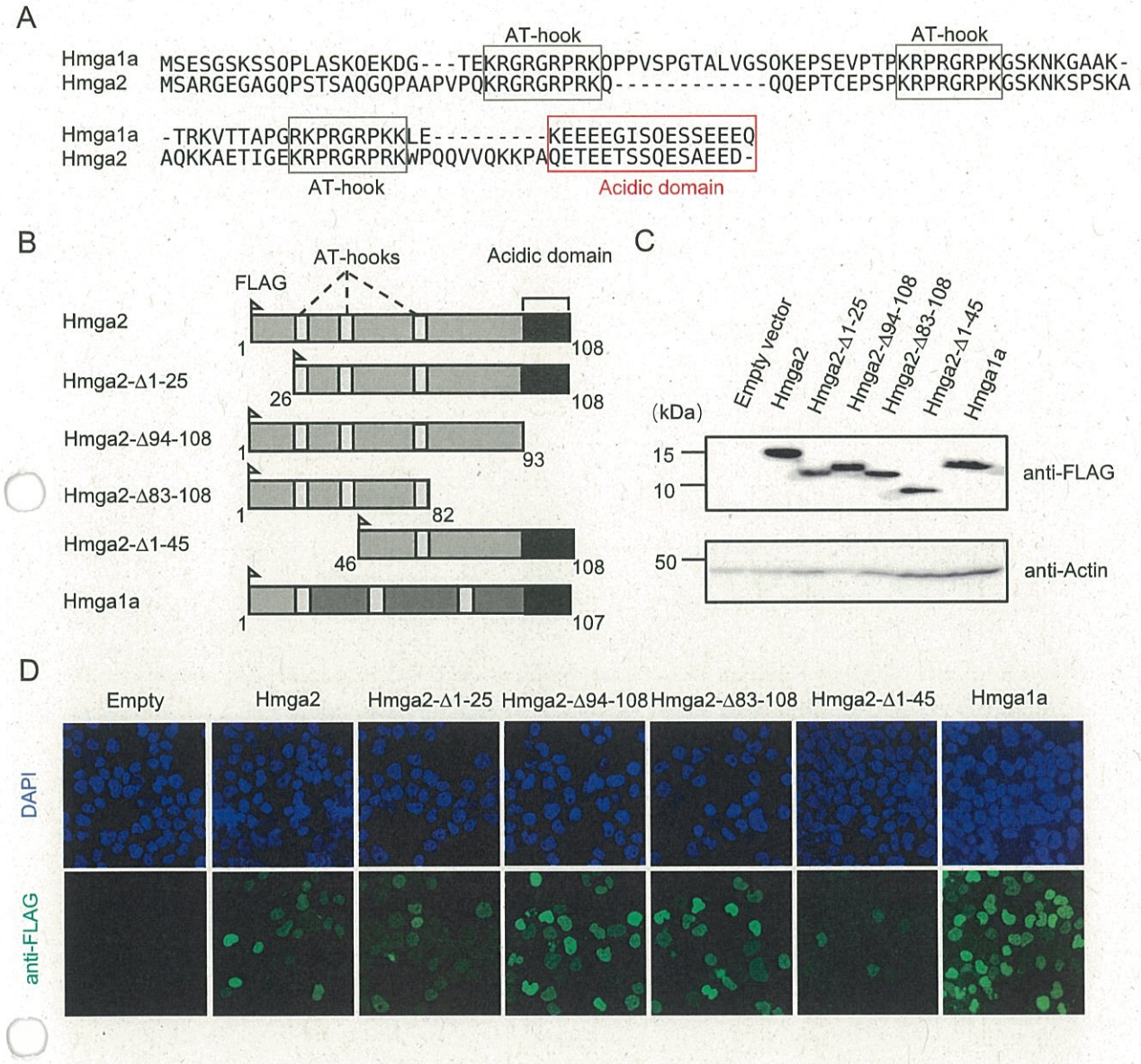
A
AT-hook
AT-hook
Hmga1a MSESGSKSSQPLASKQEKDG---TEKRGRGRPRKQPPVSPGTALVGSQKEPSEVPTPKRPRGRPKGSKNKGAAK-
Hmga2 MSARGEGAGQPSTSAQGQPAAPVPQKRGRGRPRKQ----------QQEPTCEPSPKRPRGRPKGSKNKSPSKA
Hmga1a -TRKVTTAPGRKPRGRPKKLE---------KEEEEGISQESSEEEQ
Hmga2 AQKKAETIGEKRPRGRPRKWPQQVVQKKPAQETEETSSQESAEED-
AT-hook
Acidic domain
B
AT-hooks
Acidic domain
FLAG
Hmga2
Hmga2-Δ1-25
Hmga2-Δ94-108
Hmga2-Δ83-108
Hmga2-Δ1-45
Hmga1a
1
108
26
108
1
93
1
82
46
108
1
107
C
Empty vector
Hmga2
Hmga2-Δ1-25
Hmga2-Δ94-108
Hmga2-Δ83-108
Hmga2-Δ1-45
Hmga1a
(kDa)
15
10
anti-FLAG
50
anti-Actin
D
Empty
Hmga2
Hmga2-Δ1-25
Hmga2-Δ94-108
Hmga2-Δ83-108
Hmga2-Δ1-45
Hmga1a
DAPI
anti-FLAG

Figure 5

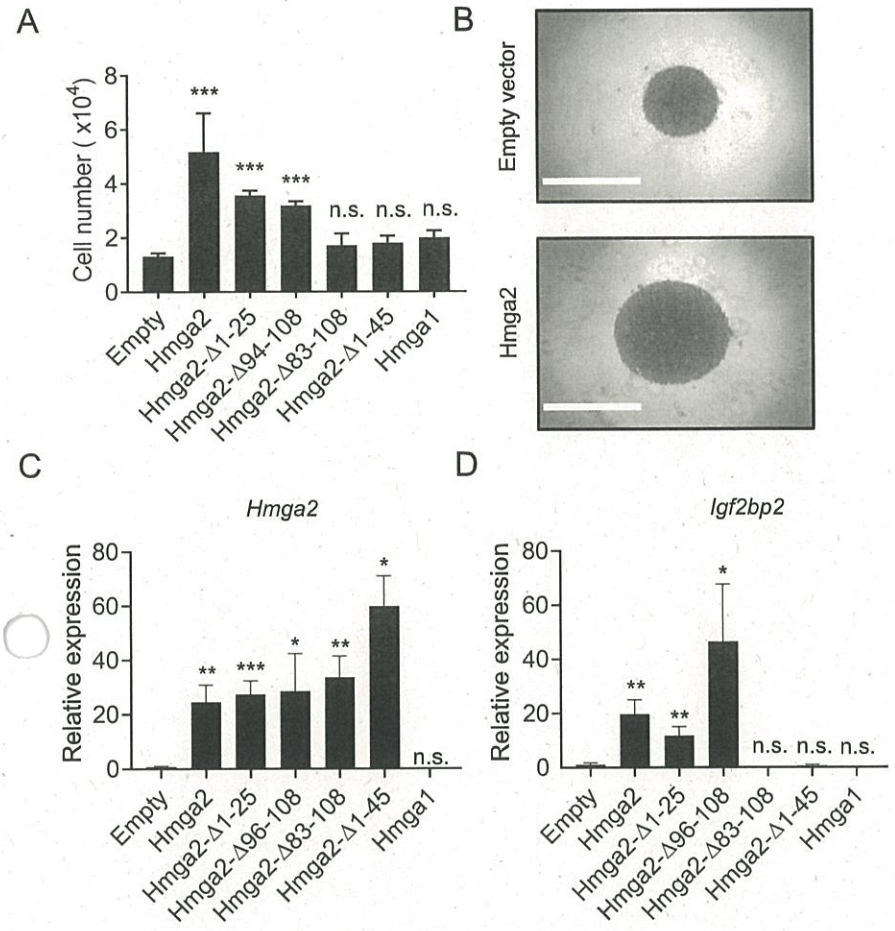
A
Cell number (x10^4)
8
6
4
2
0
***
***
***
n.s. n.s. n.s.
Empty
Hmga2
Hmga2-Δ1-25
Hmga2-Δ94-108
Hmga2-Δ83-108
Hmga2-Δ1-45
Hmga1
B
Empty vector
Hmga2
C
Hmga2
Relative expression
80
60
40
20
0
**
***
*
**
*
n.s.
Empty
Hmga2
Hmga2-Δ1-25
Hmga2-Δ96-108
Hmga2-Δ83-108
Hmga2-Δ1-45
Hmga1
D
Igf2bp2
Relative expression
80
60
40
20
0
**
**
*
n.s. n.s. n.s.
Empty
Hmga2
Hmga2-Δ1-25
Hmga2-Δ96-108
Hmga2-Δ83-108
Hmga2-Δ1-45
Hmga1